THE ASTROPHYSICAL JOURNAL, 370:559–566, 1991 April 1


# MULTICOLOR CCD IMAGING OF SUPERGIANTS IN THE DISK OF NGC 253

T. J. DAVIDGE, O. LE FÈVRE, AND C. C. CLARK
Canada-France-Hawaii Telescope Corporation, P.O. Box 1597, Kamuela, HI 96743
*Received 1990 July 2; accepted 1990 September 18*

## ABSTRACT

Using the 3.6 m Canada-France-Hawaii Telescope (CFHT), we have obtained *B*, *V*, and *R* CCD images of a large field in the nearby galaxy NGC 253, sampling portions of both the inner and outer disk regions (Scoville et al. 1985). The data were recorded during conditions of exceptionally good seeing, permitting individual stars to be resolved over a large area of the galaxy. Two-color and color-magnitude diagrams are constructed, and it appears that the majority of the stars we have detected are supergiants of spectral types A, F, and G. We find that (1) the difference in mean visual extinction between the inner and outer disk is $\sim 1$ magnitude; (2) the apparent brightnesses of the most luminous stars in the inner and outer disk regions are similar which, given the difference in mean extinction, suggests that the former area contains stars which are intrinsically brighter, and hence more massive, than in the latter; and (3) if $A_V$ does not exceed $\sim 2$ magnitudes, the majority of the stars we have detected have masses less than or equal to 40 $M_\odot$. Finally, the luminosity functions in all three bandpasses of stars in the outer disk region follow power laws, with slopes similar to those seen in other spiral galaxies. The brightest red supergiants occur at $V \sim 19.0$ and, if these stars are similar to those in other nearby galaxies, then the distance modulus of NGC 253 is less than or equal to 27.0.

*Subject headings:* galaxies: individual (NGC 253) — galaxies: photometry — galaxies: stellar content — stars: evolution — stars: supergiants

## 1. INTRODUCTION

Observations of massive stars in the Milky Way and nearby galaxies suggest that mass loss and overshooting from convective cores play important roles in defining the morphology of the most luminous regions of the H-R diagram (e.g., Chiosi & Maeder 1986, and references therein). The observational effects of mass loss and overshooting are apparent during both the main-sequence and post–main-sequence phases of evolution (e.g., Chiosi, Nasi, & Sreenivasen 1978; Bressan, Bertelli, & Chiosi 1981; Maeder 1981; Doom 1982), although what are perhaps the most conspicuous signatures of these processes are evident during the latter phase. For example, episodes of extreme mass loss, combined with the mixing to the surface of core-processed material, are thought to be responsible for (1) the absence of red supergiants (RSGs) more luminous than $M_{\rm bol} \sim -10$; (2) the progressive narrowing of those regions in the H-R diagram occupied by yellow and blue supergiants (BSGs) at luminosities in excess of $M_{\rm bol} \sim -10$; and (3) the presence of variable blue and yellow supergiants at the redward extent of stellar evolution in the upper regions of the H-R diagram (e.g., Humphreys & Davidson 1979; Humphreys et al. 1986). These results are qualitatively consistent with stellar evolution calculations which show that, if the rate of mass loss is suitably large, evolution to cooler effective temperatures can be reversed (e.g., Maeder 1981); optical variability can be a natural consequence due to rapid changes in bolometric correction (e.g., Stothers & Chin 1983). Various physical causes for the instabilities which induce the extreme mass loss rates have been considered in the literature (e.g., Lamers & Fitzpatrick 1988; de Jager 1980, 1984).

Because luminous supergiants are relatively rare, it is important to study these stars in as large a sample of nearby galaxies as possible in order to better constrain the morphology of the upper portions of the H-R diagram. Studies of luminous stars in nearby galaxies are especially important since the component stars are equidistant and, in many cases, relatively unobscured compared with their Milky Way counterparts. Data of this nature can be used to investigate the behavior of, for example, the maximum brightness of RSGs as a function of galaxy luminosity, a subject which remains a matter of controversy (e.g., Sandage & Bedke 1988; Humphreys et al. 1986). Unfortunately, studies of luminous extragalactic stars, particularly outside the Local Group, encounter a number of complications. Crowding and confusion with H II regions are certainly important considerations (e.g., Humphreys & Aaronson 1987), as are variations in the local sky background due to, for example, nebulosity. These factors can compromise both the accuracy of photometric measurements and the identification of supergiants.

Because of their close proximity, members of the so-called Sculptor Group (if it is indeed a single group—Puche & Carignan 1988; Pritchet et al. 1987) can play an important role in studies of massive stars. NGC 253 is of particular interest as it is the most luminous member of this group, and it is the nearest large spiral galaxy after M31. Furthermore, a remarkable property of NGC 253 is the intense star-forming activity in its central regions (e.g., Rieke et al. 1980). The rate of star formation in the nucleus and inner disk regions declines exponentially with radial distance from the galaxy center, with a scale length markedly smaller than that seen in other Sc galaxies (Waller, Kleinmann, & Richer 1988). Photometric mapping of NGC 253 at near-infrared wavelengths by Scoville et al. (1985) revealed three distinct components: a compact central nucleus; a constant surface-brightness inner disk, which contains a barlike structure; and an outer disk. There is also a large-scale galactic wind (McCarthy, Heckman, & van Breugel 1987), presumably originating from supernova activity in the nucleus. However, despite the obvious importance of NGC 253, there have been no published surveys of the stellar content of this galaxy. Attempts to detect Cepheids (Aaronson 1986) have apparently been unsuccessful, probably due to the large quantities of gas and dust in the disk. To our knowledge,

the only published study of individual stars in NGC 253 is that of Davidge & Pritchet (1990), who resolved asymptotic and red giant branch stars in the halo.

In the current study we discuss *B*, *V*, and *R* CCD observations of a single large field in the disk of NGC 253 obtained during sub–arcsecond seeing conditions. The observations and their reduction are described in § 2, while the methods used to measure stellar brightnesses are discussed in § 3. The data were used to construct two-color and color-magnitude diagrams, and these are presented in §§ 4 and 5, respectively. In § 6 the luminosity functions in all three bandpasses are discussed, and an upper limit to the distance to NGC 253 is estimated using the observed maximum brightness of RSGs. A summary of the results is given in § 7.

## 2. OBSERVATIONS AND DATA REDUCTION

The data were obtained at the prime focus of the 3.6 m Canada-France-Hawaii Telescope (CFHT) during the night of UT 1989 October 20. A field located roughly 5 arcminutes northeast of the galaxy nucleus, centered at $0^h45^m22^s$ right ascension and $-25°31'25''$ declination (epoch 1950), was selected for study. The data were recorded through standard *B*, *V*, and *R* (Kron-Cousins system) filters with an integration time of 400 s per bandpass. The detector used for these observations was SAIC1, a thick low-noise three-phase Ford Aerospace design CCD with 18 $\mu$m square pixels in a 1024 × 1024 format. The field of view of this detector at the CFHT prime focus is roughly 252 arcseconds per side, so that a large portion of the disk of NGC 253 could be sampled in a single exposure. The seeing, which was identical in all three filters, was measured to be ~0.7 arcseconds FWHM.

The raw data were reduced using standard CCD processing techniques. The processing sequence consisted of (1) subtraction of a median bias frame, (2) removal of bad pixels and columns, (3) division by a mean dome flat, and (4) alignment of all three images. A portion of the final *B* frame is shown in Figure 1; our field covers almost a third of the total disk of NGC 253 as seen on the Palomar Observatory Sky Survey, and includes portions of both the inner and outer disk components as described by Scoville et al. (1985).

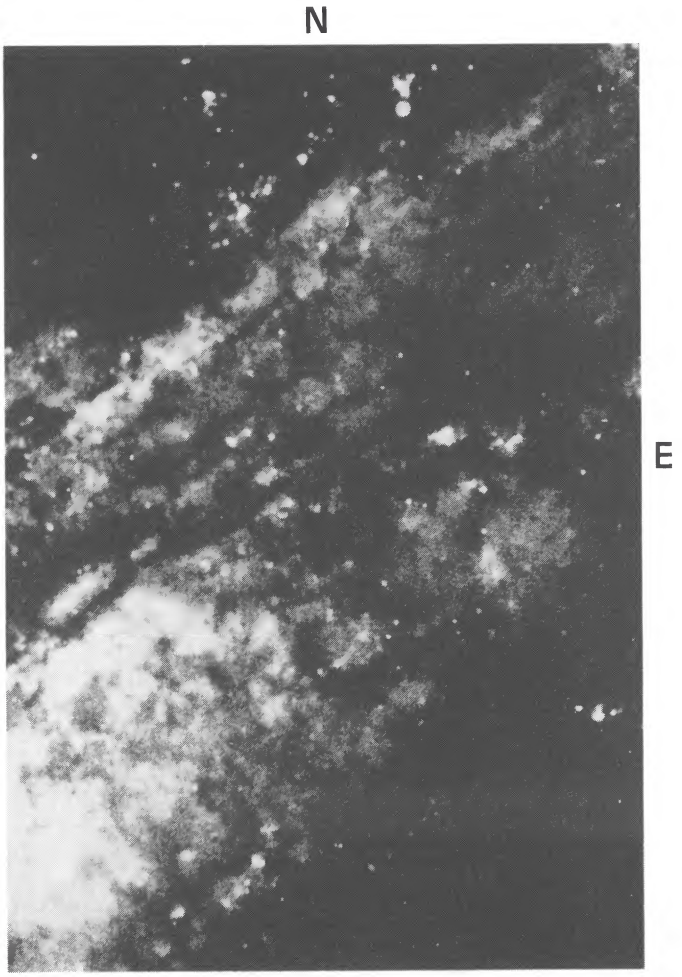


FIG. 1.—*B* CCD image of the NGC 253 disk field. North is at the top, and east is to the right.

## 3. PHOTOMETRIC MEASUREMENTS

All photometric measurements were made with CFHPHOT, a version of DAOPHOT (Stetson 1987) modified by R. McGonegal to run in the IRAF environment at CFHT. The data were calibrated using observations of standard star fields in globular clusters (Christian et al. 1985). The Galactic extinction along the line of sight to NGC 253 is negligible (Burstein and Heiles 1984), so a correction for foreground reddening was not applied.

The point spread function (PSF) fitting algorithm in the DAOPHOT routine NSTAR assumes a constant sky background in the vicinity of each star. This is not a good assumption in the disk of NGC 253, where there are significant variations due to spiral structure, H II regions, and localized areas of high extinction. Consequently, an iterative procedure, similar to that employed by Davidge & Jones (1989), Pritchet et al. (1987), and Hopp & Schulte-Ladbeck (1987), was used in an effort to reduce the effects of background variations on the photometric measurements.

A preliminary set of photometric measurements were generated with no correction for variable background, and the fitted stellar profiles were subtracted from the data using the routine SUBSTAR. The star-subtracted images were smoothed to remove artifacts of the subtraction process, and the results were then in turn subtracted from the original images. CFHPHOT was then run on the background-subtracted images to produce an improved set of measurements.

The removal of irregular background variations improved the ability of NSTAR to fit stellar profiles. This is evident from the uncertainties in the photometric measurements output by NSTAR, which reflect the quality of the PSF fit. The fitting errors were reduced, on average, by 0.05 magnitudes in *B*, and 0.03 magnitudes in *V* and *R*.

Completeness and uncertainties in the photometric measurements were determined by adding synthetic stars of known brightness to the initial data frames, rerunning CFHPHOT using the background subtraction procedure described above, and computing the recovery statistics. These experiments were distributed over a number of different runs, to prevent artificially increasing the degree of crowding. The results are summarized in Table 1, and we emphasize that the values in this table are applicable to a "typical" region in the disk, and are not appropriate for isolated dense clusters of stars (e.g., § 6).

The *B* and *V* photometric measurements are largely free of systematic effects down to ~20th magnitude; however, this is not the case in *R*, where the results in Table 1 indicate that stellar brightnesses are overestimated on average by ~0.15

TABLE 1

MAGNITUDE ERRORS AND COMPLETENESS FRACTIONS

| Filter | $m^a$ | $\Delta m^b$ | $\sigma^c$ | C[d] |
|---|---|---|---|---|
| $B$..... | 18.5 | −0.001 | 0.015 | 1.000 |
| | 19.0 | 0.001 | 0.008 | 1.000 |
| | 19.5 | 0.013 | 0.012 | 1.000 |
| | 20.0 | 0.006 | 0.021 | 1.000 |
| | 20.5 | −0.027 | 0.020 | 0.882 ± 0.055 |
| | 21.0 | −0.032 | 0.062 | 0.600 ± 0.083 |
| | 21.5 | 0.020 | 0.214 | 0.194 ± 0.071 |
| $V$..... | 18.5 | −0.004 | 0.022 | 1.000 |
| | 19.0 | −0.018 | 0.017 | 1.000 |
| | 19.5 | −0.018 | 0.021 | 1.000 |
| | 20.0 | 0.103 | 0.038 | 1.000 |
| | 20.5 | 0.081 | 0.048 | 0.933 ± 0.046 |
| | 21.0 | 0.032 | 0.077 | 0.686 ± 0.078 |
| | 21.5 | 0.159 | 0.123 | 0.372 ± 0.074 |
| | 22.0 | 0.592 | 0.274 | 0.135 ± 0.047 |
| $R$..... | 18.5 | 0.135 | 0.061 | 1.000 |
| | 19.0 | 0.134 | 0.051 | 1.000 |
| | 19.5 | 0.128 | 0.042 | 1.000 |
| | 20.0 | 0.201 | 0.059 | 1.000 |
| | 20.5 | 0.148 | 0.067 | 0.970 ± 0.030 |
| | 21.0 | 0.174 | 0.085 | 0.889 ± 0.047 |
| | 21.5 | 0.370 | 0.138 | 0.743 ± 0.074 |
| | 22.0 | 0.824 | 0.243 | 0.292 ± 0.093 |

[a] Actual magnitude.
[b] Actual magnitude − measured magnitude.
[c] Standard error of the mean.
[d] Completeness.

magnitudes in the range $18.5 \geq R \geq 20.5$. This effect does not appear to vary with position on the frame, and we cannot offer an unambiguous explanation for its cause, although we suspect that NSTAR systematically underestimated the $R$ band sky values. In any event, a correction factor of 0.15 magnitudes was applied to the $R$ data to account for this systematic effect, and the corrected data matches fiducial stellar sequences in the two-color diagram very well (§ 4).

## 4. THE TWO-COLOR DIAGRAM

The CCD images cover two of the three regions of the NGC 253 disk described by Scoville et al. (1985): (1) the inner disk, which is seen in the lower left-hand corner of Figure 1 and contains many compact H II regions and clusters of supergiants, and (2) the outer disk, which occupies the bulk of our field and has a substantially lower surface density of bright supergiants. We consider these regions separately in the subsequent discussion.

The two-color diagrams of the inner and outer disk regions are shown in Figures 2 and 3; the sequence expected for Galactic supergiants is also shown for comparison. The Galactic supergiant sequence was derived from data tabulated by FitzGerald (1970) for $B-V$ and Johnson (1966) for $V-R$; the latter measurements were converted into the Kron-Cousins system using transformation equations from Bessell (1979). The NGC 253 observations scatter more-or-less uniformly about the Galactic supergiant sequence; the agreement would be much worse if a correction factor for systematic effects in the $R$ data had not been applied (§ 3). Based on Figures 2 and 3, it appears that the majority of the objects detected in all three colors are supergiants of spectral types A, F, and G.

We suspect that some, but not all, of the stars we have detected are heavily reddened, as the disk of NGC 253 contains large quantities of gas and dust. Waller et al. (1988) used the relative strengths of the [S III]λ9532 and Hα lines to estimate extinction toward embedded H II regions in the disk of NGC 253, and the results indicate that at a distance of ~200″ from the nucleus, corresponding to the center of our outer disk field, $A_V \sim 4$ magnitudes, whereas at a radial distance of ~100″, which is the beginning of the inner disk component, $A_V \sim 5$ magnitudes. We consider these values of $A_V$ to be extreme upper limits for our sample, as an imaging survey for bright stars at optical wavelengths will be biased toward unreddened sources.

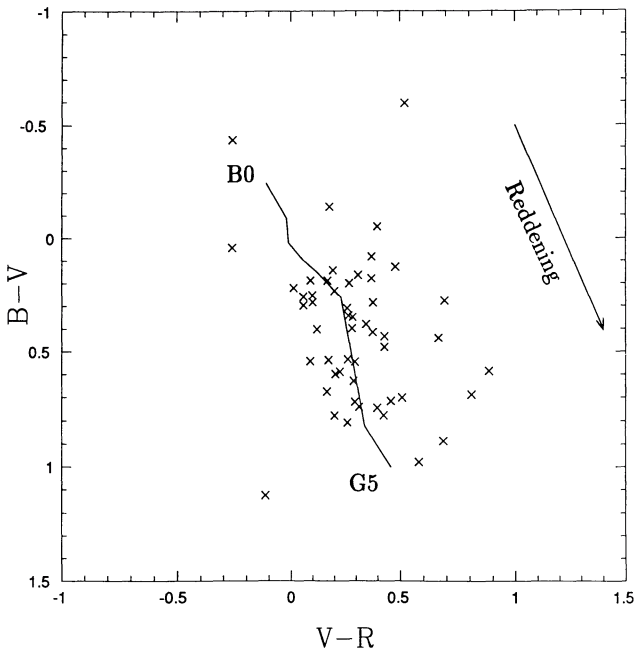


FIG. 2.—Two-color diagram of the inner disk region. Also shown is the sequence expected for Galactic supergiants (see text) spanning spectral types B0 to G5. The reddening vector is also indicated.

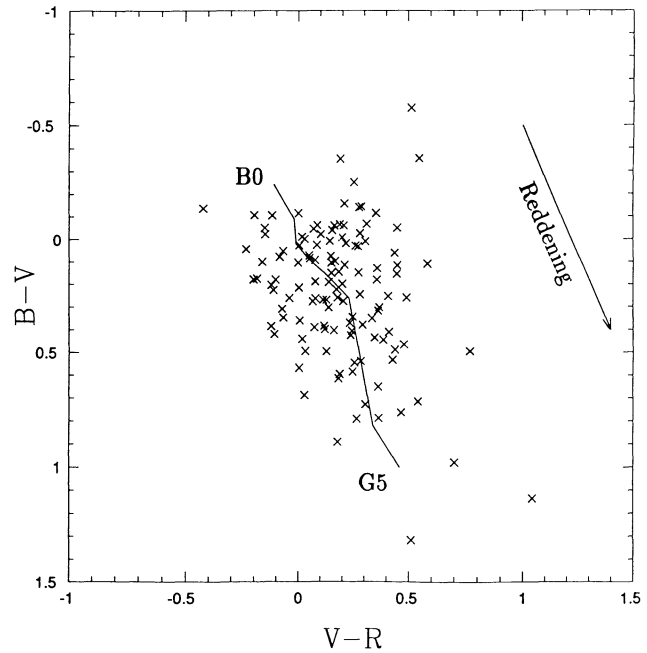


FIG. 3.—Same as Fig. 2, except for the outer disk region

A reddening vector, derived from observations of LMC supergiants (Grieve & Madore 1986), is shown in Figures 2 and 3. The reddening vector parallels the stellar sequence, so it is difficult to establish unambiguously the amount of reddening for individual stars from the two-color diagram alone. However, if the stellar contents of the inner and outer disk regions are assumed to be similar, then the mean *difference* in extinction between the stars in the two areas can be estimated. The two-color diagrams of the inner and outer disk regions differ in that the main body of data from the outer disk extends to bluer $B-V$ and $V-R$ colors than that from the inner disk. If the bluest stars in the inner disk are assumed to have identical intrinsic colors to those in the outer disk, then the net difference in $B-V$ color excess is $\Delta E(B-V) \sim 0.3$, corresponding to $\Delta A_V \sim 1$ magnitude. This value is in good agreement with that expected from Waller et al. (1988).

### 5. THE COLOR-MAGNITUDE DIAGRAMS OF THE INNER AND OUTER DISK REGIONS

The color-magnitude diagrams (CMDs) of the inner and outer disk regions are shown in Figures 4 through 7. In both regions the dominant feature is a concentration of stars at intermediate colors, which we identify as supergiants of spectral types A, F, and G. The main concentration of these stars in the CMD of the inner disk occurs at slightly redder colors than the outer disk, a result which we attribute to differential extinction (§ 3). RSGs, which we define to have spectral-types later than K0 ($B-V \sim 1.2$, $V-R \sim 0.5$), are also present in both regions. The upper envelopes defined by the brightest stars in the CMDs of both regions are similar, although the relative distributions of the inner and outer disk stars in the CMDs are very different. In particular, whereas the majority of stars in the outer disk fall below the 20 $M_\odot$ evolutionary track (see below), the distribution of inner disk stars in the CMDs is much more uniform. This difference may reflect the larger photometric uncertainties and smaller completeness fractions in crowded environments. Given that the stars in the inner disk are probably more heavily reddened than those in the outer disk but have similar apparent magnitudes, the most luminous BSGs in the former region are intrinsically brighter, and hence more massive, than those in the latter.

The 20 and 40 $M_\odot$ evolutionary tracks of Maeder & Meynet (1988, 1989) have been translated onto the CMDs using the effective temperature and bolometric correction calibrations of Humphreys & McElroy (1984) and assuming $\mu_0 = 27.0$ (Puche

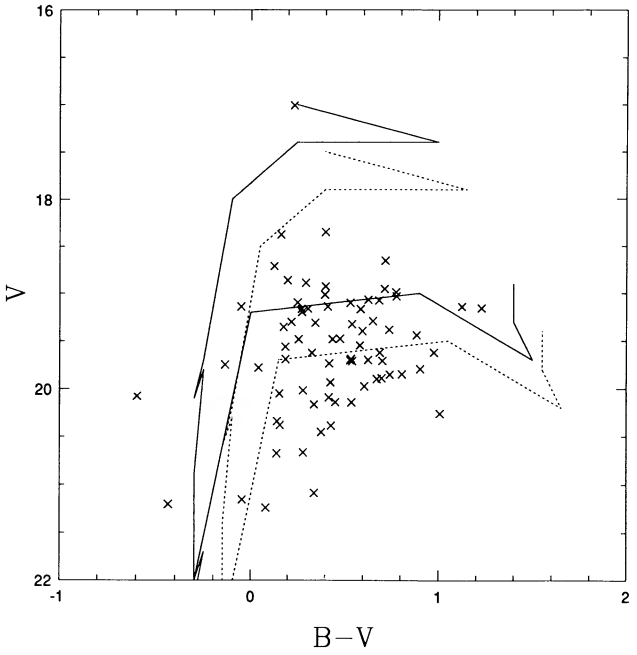


FIG. 4.—$V$, $B-V$ color-magnitude diagram for the inner disk region. Also shown are the 20 $M_\odot$ and 40 $M_\odot$ evolutionary tracks of Maeder & Meynet (1988, 1989) for no extinction (*solid line*) and $E(B-V) = 0.15$ (*dashed line*). A distance modulus of 27.0 has been assumed.

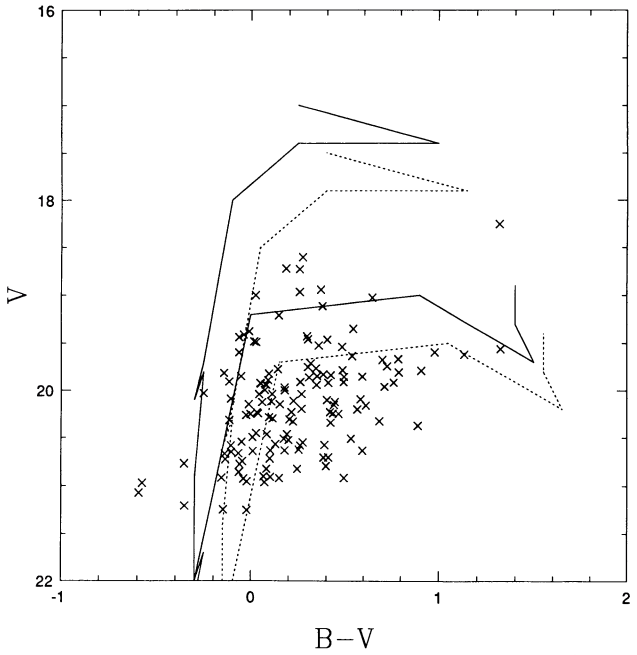


FIG. 5.—Same as Fig. 4, except for the outer disk region

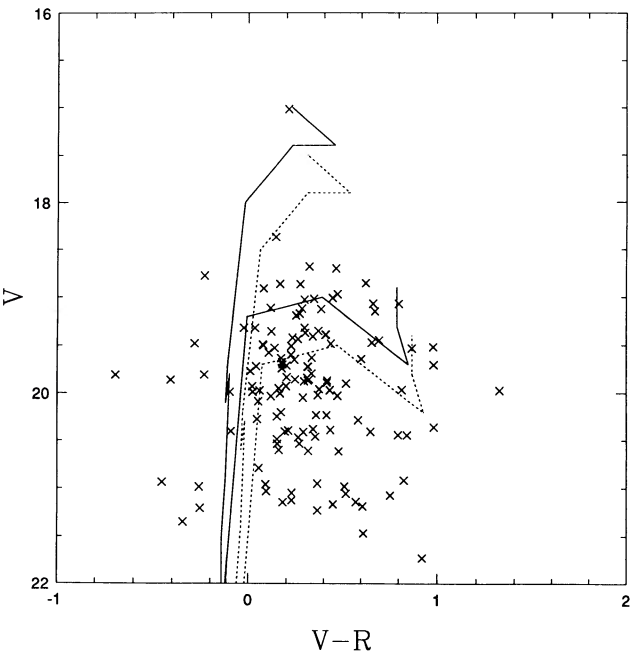


FIG. 6.—$V$, $V-R$ color-magnitude diagram of stars in the inner disk

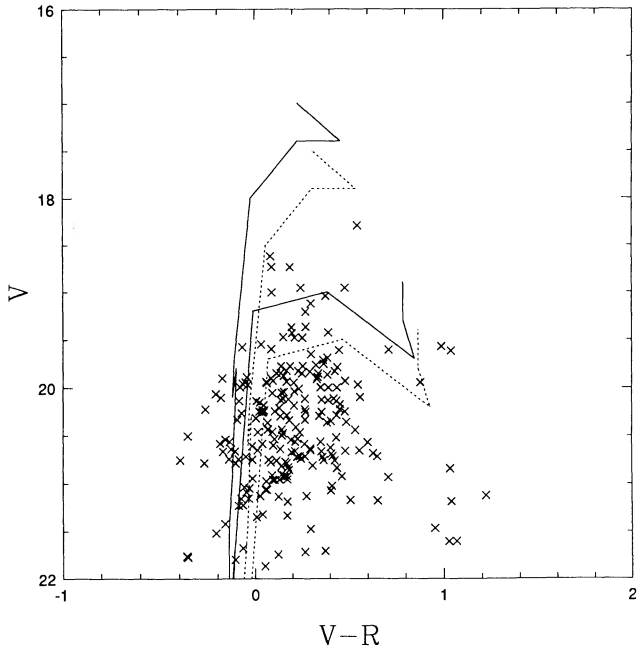


FIG. 7.—$V$, $V-R$ color-magnitude diagram of stars in the outer disk region

& Carignan 1988), a value which we adopt for all subsequent calculations. Calibrations relating color and spectral type were taken from FitzGerald (1970) for $B-V$, and Johnson (1966) for $V-R$, after appropriate relations from Bessell (1979) were used to transform the measurements into the Kron-Cousins system. The evolutionary tracks shown as solid lines in these figures assume no reddening, while those shown as dashed lines assume $E(B-V) \sim 0.15$, corresponding to roughly half a magnitude of visual extinction.

Based on Figures 4–7, the majority of stars in both the inner and outer disk regions appear to have initial masses below 40 $M_\odot$, if $A_V$ does not exceed $\sim$1–2 magnitudes. The apparent absence of very massive stars is surprising since supergiants with $M \geq 40\ M_\odot$ are not uncommon in other nearby galaxies (e.g., Blaha & Humphreys 1989). Possible explanations for this discrepancy are that (1) stars more massive than 40 $M_\odot$ may be heavily obscured in the disk of NGC 253, with $A_V$ in excess of $\sim$2 magnitudes, such that they are either undetected or appear fainter and redder than they would in other galaxies; (2) star formation may have terminated a few million years ago; or (3) the initial mass function (IMF) in NGC 253 is such that these stars do not form. Given the heavy extinction seen toward H II regions in the disk of NGC 253 (Waller et al. 1988), we suspect that the first explanation is correct, although we cannot unambiguously rule out the second or third possibility with the existing data.

The ratio of luminous blue and red supergiants, B/R, has been derived from the photometric observations by estimating spectral types for each star based on the observed $V-R$ color. Absolute bolometric magnitudes were then calculated using bolometric corrections from Humphreys & McElroy (1984). This procedure produces inaccurate bolometric luminosities when $V-R \leq 0.0$, as the bolometric correction changes very rapidly in this region. However, only a small portion of our data falls in this color range. After applying completeness corrections, we find that in the interval $-8.5 \leq M_{\rm bol} \leq -7.5$ B/R is $\sim$1–4. This result does not change if small shifts are applied to $V-R$ to account for systematic effects in the photometry (§ 3). Humphreys & McElroy (1984) found that among supergiants of similar luminosity B/R is $\sim$20–30 in the solar neighborhood, $\sim$7 in the LMC, and $\sim$4 in the SMC. Therefore, in the particular field we have observed, the photometrically determined B/R is substantially smaller than in the solar neighborhood and is comparable to that in the SMC (Humphreys & McElroy 1984).

The low value of B/R is qualitatively consistent with the absence of extremely massive stars, since B/R is a decreasing function of mass (e.g., Maeder & Meynet 1988). However, a significant population of heavily reddened BSGs could also artificially lower photometric estimates of B/R, as stars of this nature will have apparent photometric properties similar to RSGs. Spectroscopic observations of luminous stars in the disk of NGC 253 will be necessary to assess the extent to which heavily reddened BSGs contaminate the region of the H-R diagram occupied by RSGs.

## 6. THE $B$, $V$, AND $R$ LUMINOSITY FUNCTIONS AND THE DISTANCE TO NGC 253

The $B$, $V$, and $R$ luminosity functions of stars in the outer disk are given in Tables 2, 3, and 4, and shown in Figures 8, 9, and 10. We have not constructed luminosity functions for stars in the inner disk because of the small number of objects detected in this region. It is apparent from Figures 8 through 10 that the luminosity functions, corrected for completeness using the results from Table 1, follow power laws at the bright end, a result consistent with what is seen in other galaxies (e.g., Blaha & Humphreys 1989; Freedman 1985; Hoessel 1985). In

TABLE 2

$B$ OUTER DISK LUMINOSITY FUNCTION

| $B$ | log $(n)$[a] | log $(n_c)$[b] |
|---|---|---|
| 17.5..... | $0.70^{+0.16;-0.26}$ | $0.70^{+0.16;-0.26}$ |
| 18.0..... | $0.85^{+0.13;-0.21}$ | $0.85^{+0.13;-0.21}$ |
| 18.5..... | $1.08^{+0.11;-0.15}$ | $1.08^{+0.11;-0.15}$ |
| 19.0..... | $1.46^{+0.08;-0.09}$ | $1.46^{+0.08;-0.09}$ |
| 19.5..... | $1.77^{+0.05;-0.06}$ | $1.77^{+0.05;-0.06}$ |
| 20.0..... | $2.01^{+0.04;-0.04}$ | $2.01^{+0.04;-0.04}$ |
| 20.5..... | $2.17^{+0.03;-0.04}$ | $2.22^{+0.04;-0.04}$ |
| 21.0..... | $2.17^{+0.03;-0.04}$ | $2.39^{+0.07;-0.07}$ |
| 21.5..... | $2.15^{+0.03;-0.04}$ | $2.86^{+0.14;-0.20}$ |

[a] Number of stars detected per magnitude interval.
[b] Number of stars detected per magnitude interval corrected for completeness.

TABLE 3

$V$ OUTER DISK LUMINOSITY FUNCTION

| $V$ | log $(n)$[a] | log $(n_c)$[b] |
|---|---|---|
| 17.5..... | $0.00^{+0.30;-\infty}$ | $0.00^{+0.30;-\infty}$ |
| 18.0..... | $0.48^{+0.20;-0.38}$ | $0.48^{+0.20;-0.38}$ |
| 18.5..... | $1.00^{+0.12;-0.17}$ | $1.00^{+0.12;-0.17}$ |
| 19.0..... | $1.36^{+0.08;-0.10}$ | $1.36^{+0.08;-0.10}$ |
| 19.5..... | $1.81^{+0.05;-0.06}$ | $1.81^{+0.05;-0.06}$ |
| 20.0..... | $2.17^{+0.03;-0.04}$ | $2.17^{+0.03;-0.04}$ |
| 20.5..... | $2.37^{+0.03;-0.03}$ | $2.40^{+0.04;-0.04}$ |
| 21.0..... | $2.33^{+0.03;-0.03}$ | $2.50^{+0.05;-0.06}$ |
| 21.5..... | $2.20^{+0.03;-0.03}$ | $2.63^{+0.09;-0.10}$ |
| 22.0..... | $2.17^{+0.03;-0.04}$ | $3.04^{+0.13;-0.20}$ |

[a] Number of stars detected per magnitude interval.
[b] Number of stars detected per magnitude interval corrected for completeness.

TABLE 4

*R* Outer Disk Luminosity Function

| *R* | log (*n*)[a] | log ($n_c$)[b] |
|---|---|---|
| 17.5..... | $0.00^{+0.30;-\infty}$ | $0.00^{+0.30;-\infty}$ |
| 18.0..... | $0.90^{+0.13;-0.19}$ | $0.90^{+0.13;-0.19}$ |
| 18.5..... | $1.30^{+0.09;-0.11}$ | $1.30^{+0.09;-0.11}$ |
| 19.0..... | $1.71^{+0.05;-0.07}$ | $1.71^{+0.05;-0.07}$ |
| 19.5..... | $2.09^{+0.04;-0.04}$ | $2.09^{+0.04;-0.04}$ |
| 20.0..... | $2.46^{+0.03;-0.03}$ | $2.46^{+0.03;-0.03}$ |
| 20.5..... | $2.71^{+0.02;-0.02}$ | $2.73^{+0.03;-0.03}$ |
| 21.0..... | $2.78^{+0.02;-0.02}$ | $2.83^{+0.03;-0.03}$ |
| 21.5..... | $2.69^{+0.02;-0.02}$ | $2.82^{+0.04;-0.05}$ |
| 22.0..... | $2.52^{+0.02;-0.02}$ | $3.06^{+0.12;-0.17}$ |

[a] Number of stars detected per magnitude interval.
[b] Number of stars detected per magnitude interval corrected for completeness.

the magnitude intervals where the completeness corrections are small, the slopes of the *V* and *R* luminosity functions are similar, although the *B* luminosity function is flatter than the other two. In the interval $17.5 \leq M \leq 20.0$, the slopes of the luminosity functions are $0.56 \pm 0.03$ (*B*), $0.87 \pm 0.06$ (*V*), and $0.93 \pm 0.17$ (*R*). These values are consistent with what is seen in the Milky Way and other nearby galaxies (e.g., Blaha & Humphreys 1989; Freedman 1985). At faint magnitudes, there is a tendency, which is most pronounced in *R*, for the luminosity functions to deviate from a simple power law. We suspect that this is not a real effect, but may result from shortcomings in the completeness experiments, which were performed over a large area of the disk, and hence cannot account for the effects of crowding in isolated compact star clusters and associations.

The current observations can be used to estimate the distance to NGC 253 based on the brightest blue and red supergiants. BSGs and RSGs are potentially useful distance indicators since they are extremely bright ($M_v \sim -8$ to $-10$); however, these stars can have variable light output, and contamination from faint foreground stars can also be a problem. The latter consideration is especially important for RSGs, since the majority of foreground stars have red colors.

A potentially serious difficulty with the use of BSGs as distance indicators is that the brightness calibration is sensitive to galaxy mass and variations in the star formation history. These

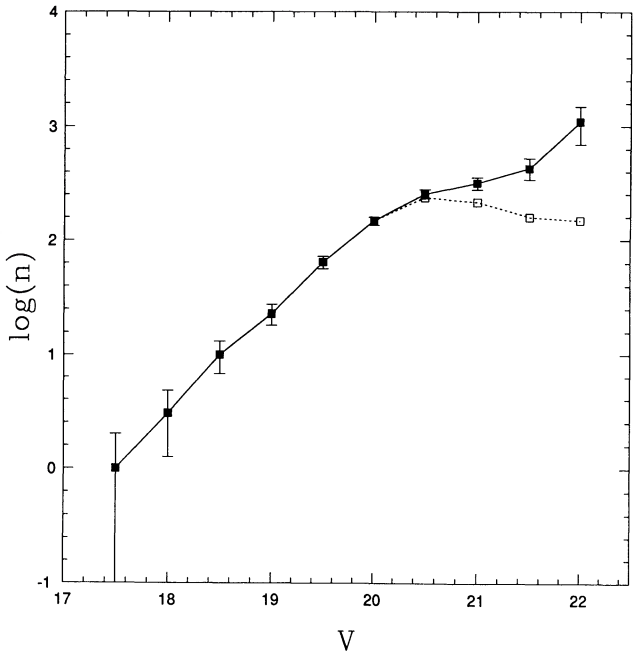


FIG. 9.—*V* luminosity function of stars in the outer disk region. The solid line is the luminosity function corrected for incompleteness using the results from Table 1.

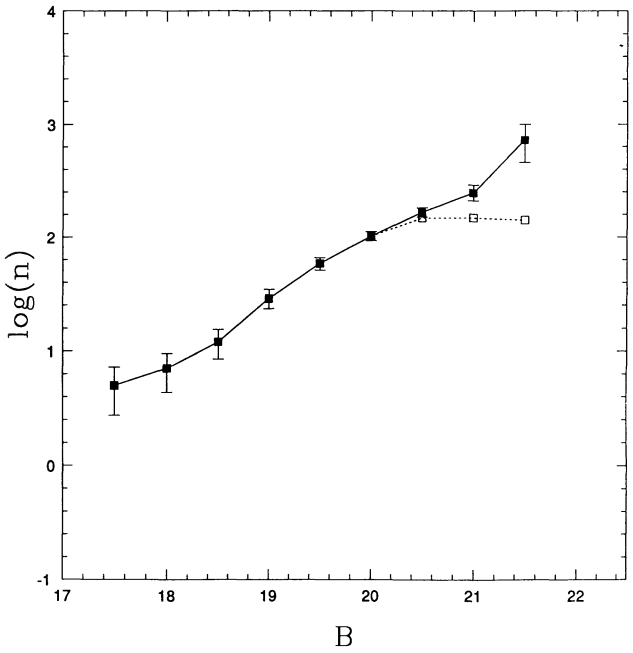


FIG. 8.—*B* luminosity function of stars in the outer disk region. The solid line is the luminosity function corrected for incompleteness using the results from Table 1.

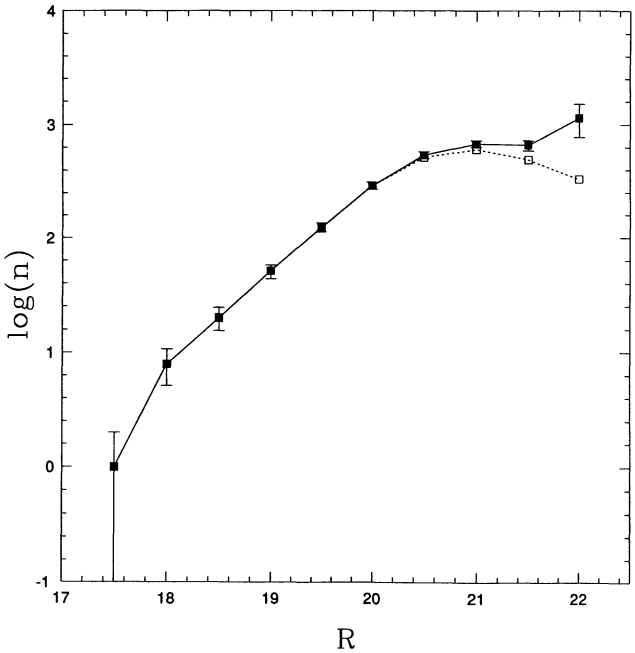


FIG. 10.—*R* luminosity function of stars in the outer disk region. The solid line is the luminosity function corrected for incompleteness using the results from Table 1.

factors are thought to be responsible for the empirical relation seen between maximum BSG brightness and integrated galaxy luminosity (de Vaucouleurs 1978a; Sandage & Tammann 1982; Humphreys 1983); rare, massive stars are expected to occur with a higher frequency in giant galaxies than dwarf galaxies because the absolute star formation rate in the former is substantially higher than in the latter. However, unlike the case for BSGs, there appears to be a well-defined maximum brightness for RSGs which spans a large range of integrated galaxy luminosity (Humphreys & Davidson 1979; Sandage & Tammann 1982; but see also Sandage 1984 and Sandage & Bedke 1988), a result which may be explained based on current ideas of massive star evolution (Humphreys et al. 1986; Humphreys 1983).

Crowding, confusion with H II regions, and the tendency for supergiants to occur in regions of high extinction can also compromise distances derived from BSGs, especially when observed in galaxies outside the Local Group. For example, spectroscopic observations of the brightest BSG candidates in NGC 2403, M81, and M101 by Humphreys & Aaronson (1987) revealed many to be blended images or compact H II regions. We note that unresolved star clusters could explain the flattening of the $B$ luminosity function of NGC 253 at the bright end (Fig. 8).

The brightest portion of the observed BSG luminosity function (i.e., the luminosity function for supergiants with $V-R < 0.5$) in the combined inner and outer disk regions of NGC 253 is tabulated in Table 5. The foreground star luminosity function computed from the field 1 model of Bahcall & Soneira (1981) is also shown for comparison. The blue ($B-V \leq 0.8$) and red ($B-V \geq 0.8$) foreground star entries in this table were computed from the Bahcall & Soneira (1981) results assuming a ratio of blue to red stars of $\sim 0.7$, the value expected for foreground stars in the interval $18 \leq V \leq 20$ along the line of sight to the globular cluster NGC 288, which lies close to NGC 253 on the sky (Ratnatunga & Bahcall 1985).

The number of BSGs exceeds that of blue foreground stars near $V \sim 18.5$, a result which is insensitive to small shifts in $V-R$ color to account for systematic trends in the photometry (§ 3). The integrated absolute $B$ magnitude for NGC 253 is roughly $-19.5$ (Puche & Carignan 1988), and hence the calibration of Sandage & Tammann (1982) and Humphreys (1983) indicates that the brightest BSGs should have $M_V \sim -9.5$. Therefore, the inferred BSG distance modulus for NGC 253 is $\sim 28.0$. This value is an upper limit, since (1) only a single field has been observed, and more luminous BSGs could be present in other regions of the galaxy, and (2) no correction has been made for extinction in the disk of NGC 253. Because of the dependence of the BSG brightness calibration on star formation history, we suggest that a formal distance estimate for NGC 253 based on BSGs should await a more thorough survey of a larger portion of the galaxy. A survey at near-infrared wavelengths would be especially useful, as this would reduce the effects of extinction in the galactic disk.

A RSG luminosity function was constructed for those stars with $V-R > 0.5$, and the results are tabulated in Table 5. As was the case with BSGs, data in both the inner and outer disk regions were combined. Using a bin size of 0.5 magnitudes, a statistically significant excess with respect to foreground stars occurs near $V \sim 19.0$; three stars have been detected with $19.0 \leq V \leq 19.2$. The results are insensitive to small shifts in $V-R$ color. If it is assumed that the brightest RSGs in NGC 253 have $M_V \sim -8$ (Humphreys et al. 1986; Sandage 1984; Humphreys 1983), then the distance modulus is $\sim 27.0$. As was the case for the distance derived from the BSG luminosity function, we consider this to be an upper limit, primarily because we have not corrected for extinction in the disk of NGC 253. We note that this result is in good agreement with the distance determined from bright halo giants (Davidge & Pritchet 1990) and places NGC 253 slightly closer than most previous distance estimates (e.g., Puche & Carignan 1988; Aaronson, Mould, & Huchra 1980; de Vaucouleurs 1978b), which utilized the large-scale properties of the galaxy as distance indicators. We emphasize that surveys of a larger area, preferably at near-infrared wavelengths, would be useful to further constrain the upper limit of RSGs in NGC 253.

TABLE 5

RED AND BLUE SUPERGIANT LUMINOSITY FUNCTIONS

| $V$ | $n_f$[a] | $n_{f\text{-red}}$[b] | $n_{f\text{-blue}}$[c] | $n_{RSG}$[d] | $n_{BSG}$[e] |
|---|---|---|---|---|---|
| 18.5..... | $2.5 \pm 1.6$ | $1.5 \pm 1.0$ | $1.0 \pm 0.6$ | $2 \pm 2$ | $10 \pm 5$ |
| 19.0..... | $2.9 \pm 1.7$ | $1.7 \pm 1.0$ | $1.2 \pm 0.7$ | $8 \pm 4$ | $28 \pm 8$ |
| 19.5..... | $3.3 \pm 1.8$ | $2.0 \pm 1.1$ | $1.3 \pm 0.7$ | $18 \pm 6$ | $78 \pm 13$ |
| 20.0..... | $3.8 \pm 2.0$ | $2.3 \pm 1.2$ | $1.5 \pm 0.8$ | $12 \pm 5$ | $158 \pm 18$ |

[a] Number of foreground stars integrated over all colors predicted from the field 1 model of Bahcall & Soneira 1981.
[b] Number of red foreground stars (see text for details).
[c] Number of blue foreground stars (see text for details).
[d] Number of RSGs in NGC 253.
[e] Number of BSGs in NGC 253.

## 7. SUMMARY

We have obtained $B$, $V$, and $R$ CCD images of a field in the northern disk of NGC 253, covering portions of both the inner and outer disk components. We find that the CMDs of the inner and outer disk regions contain similar features—a concentration of BSGs of spectral type A, F, and G fainter than $V \sim 18.5$, as well as a population of RSGs. The mean extinction in the inner disk appears to be higher than that in the outer disk. Comparison with evolutionary tracks indicate that most of the stars we have detected in the inner and outer disk regions have masses less than or equal to 40 $M_\odot$, suggesting that extremely massive stars are either heavily reddened or entirely abscent. The outer disk luminosity functions in all three bandpasses follow power laws, with exponents similar to those observed in other galaxies. The brightest BSGs in our field occur near $V \sim 18.5$, while the brightest RSGs occur near $\sim 19.0$. Using the latter value, we find that the distance modulus of NGC 253 is less than or equal to 27.0.

It is a pleasure to thank Richard Varian of the Scientific Applications International Corporation (SAIC), who arranged the loan of the detector used in this study, and an anonymous referee, who made numerous helpful comments which improved an earlier draft of this paper.

## REFERENCES


Aaronson, M. 1986, in Galaxy Distances and Deviations from the Universal Expansion, ed. B. F. Madore & R. B. Tully (Dordrecht: Reidel), 55
Aaronson, M., Mould, J., & Huchra, J. 1980, ApJ, 237, 655
Bahcall, J. N., & Soneira, R. M. 1981, ApJS, 47, 357
Bessell, M. S. 1979, PASP, 91, 589
Blaha, C., & Humphreys, R. M. 1989, ApJ, 98, 1598
Bressan, A. G., Bertelli, G., & Chiosi, C. 1981, A&A, 102, 25
Burstein, D., & Heiles, C. 1984, ApJS, 54, 33
Chiosi, C., & Maeder, A. 1986, ARAA, 24, 329
Chiosi, C., Nasi, E., & Sreenivasan, S. R. 1978, A&A, 63, 103
Christian, C. A., Adams, M., Barnes, J. V., Butcher, H., Hayes, D. S., Mould, J. R., & Siegel, M. 1985, PASP, 97, 363
Davidge, T. J., & Jones, J. H. 1989, AJ, 97, 1607
Davidge, T. J., & Pritchet, C. J. 1990, AJ, 100, 102
de Jager, C. 1980, The Brightest Stars (Dordrecht: Reidel)
———. 1984, A&A, 138, 246
de Vaucouleurs, G. 1987a, ApJ, 224, 14
———. 1987b, ApJ, 224, 710
Doom, C. 1982, A&A, 116, 303
FitzGerald, M. P. 1970, A&A, 4, 234
Freedman, W. L. 1985, ApJ, 299, 74
Grieve, G. R., & Madore, B. F. 1986, ApJS, 62, 427
Hoessel, J. G. 1985, in Luminous Stars and Associations in Galaxies, ed. C. W. H. de Loore, A. J. Willis, & P. Laskarides (Dordrecht: Reidel), 439
Hopp, U., & Schulte-Ladbeck, R. E. 1987, A&A, 188, 5
Humphreys, R. M. 1983, ApJ, 269, 335
Humphreys, R. M., & Aaronson, M. 1987, ApJ, 318, L69
Humphreys, R. M., Aaronson, M., Lebofsky, M., McAlary, C. W., Strom, S. E., & Capps, R. W. 1986, AJ, 91, 808
Humphreys, R. M., & Davidson, K. 1979, ApJ, 232, 409
Humphreys, R. M., & McElroy, D. B. 1984, ApJ, 284, 565
Johnson, H. L. 1966, ARAA, 4, 193
Lamers, H. J. G. L. M., & Fitzpatrick, E. L. 1988, ApJ, 324, 279
Maeder, A. 1981, A&A, 102, 401
Maeder, A., & Meynet, G. 1988, A&AS, 76, 411
———. 1989, A&A, 210, 155
McCarthy, P. J., Heckman, T., & van Breugel, W. 1987, AJ, 92, 264
Pritchet, C. J., Richer, H. B., Schade, D., Crabtree, D., & Yee, H. K. C. 1987, ApJ, 323, 79
Puche, D., & Carignan, C. 1988, AJ, 95, 1025
Pylyser, E., Doom, C., & de Loore, C. 1985, A&A, 148, 379
Ratnatunga, K. U., & Bahcall, J. N. 1985, ApJS, 59, 63
Rieke, G. H., Lebofsky, M. J., Thompson, R. I., Low, F. J., & Tokunaga, A. 1980, ApJ, 233, 24
Sandage, A. 1984, AJ, 89, 621
Sandage, A., & Bedke, J. 1988, Atlas of Galaxies Useful for Measuring the Cosmological Distance Scale (Washington: NASA)
Sandage, A., & Tammann, G. A. 1982, ApJ, 256, 339
Scoville, N. Z., Soifer, B. T., Neugebauer, G., Young, J. S., Matthews, K., & Yerka, J. 1985, ApJ, 289, 129
Stetson, P. B. 1987, PASP, 99, 191
Stothers, R., & Chin, C.-W. 1983, ApJ, 264, 583
Waller, W. H., Kleinmann, S. G., & Richer, G. R. 1988, AJ, 95, 1057